Earthq Eng & Eng Vib (2023) 22: 921-935 **DOI**: https://doi.org/10.1007/s11803-023-2216-6

Prediction of ground-borne vibration induced by impact pile driving: numerical approach and experimental validation

A. Colaço[1†], P. Alves Costa[1‡], C. Ferreira[1‡], C. Parente[1§] and J. Fernandez-Ruiz[2‡]

1. *CONSTRUCT-FEUP, University of Porto, Rua Dr. Roberto Frias, 4200-465 Porto, Portugal*

2. *University of La Coruña, Department of Civil Engineering, Campus de Elviña 15071, La Coruña, Spain*

Abstract: Deep foundations are currently used in engineering practice to solve problems caused by weak geotechnical characteristics of the ground. Impact pile driving is an interesting and viable solution from economic and technical points of view. However, it is necessary to ensure that the environmental drawbacks, namely ground-borne vibration, are adequately met. For this purpose, the authors propose an axisymmetric finite element method-perfectly matched layer (FEM-PML) approach, where the nonlinear behavior of the soil is addressed through an equivalent linear methodology. Given the complexity of the problem, an experimental test site was developed and fully characterized. The experimental work comprised in-situ and laboratory soil characterization, as well as the measurement of vibrations induced during pile driving. The comparison between experimental and numerical results demonstrated a very good agreement, from which it can be concluded that the proposed numerical approach is suitable for the prediction of vibrations induced by impact pile driving. The experimental database is available as supplemental data and may be used by other researchers in the validation of their prediction models.

Keywords: pile driving; ground-borne vibrations; numerical modeling; experimental validation

1 Introduction

Nowadays, the world population is close to 7.3 billion people, of which around 55% live in urban areas. United Nations projections estimate that the gradual shift of the human population from rural to urban areas combined with the overall growth of the world′s population could add another 2.5 billion people to urban areas by 2050. This demographic evolution creates great pressure on the construction industry, with a growing need for land occupation, typically where soils with weak geotechnical properties are predominant. Consequently, an increase in the complexity of the design and construction of building foundations is expected, since indirect foundations will be more frequently required.

The sustainable evolution of construction activities is intrinsically linked with an increase in quality demands, a decrease in construction time and a reduction of environmental impact, where the application of precast solutions plays a key role. In the specific case of deep foundations, the use of precast solutions implies pile driving. This traditional foundation technique has been subjected to several improvements over time, being now possible to drive larger and longer piles, even crossing medium dense/stiff soil layers (FHWA, 2016). However, the large-scale application of the technique in an urban environment can be conditioned, not by the technical impossibility of pile driving, but mainly by the potential consequences on the surrounding environment. In fact, pile driving requires a considerable transfer of energy to the ground (Auersch and Said, 2010), which generates vibrations that may disturb the regular operation of sensitive equipment, the quality of people′s lives and, in more extreme situations, cause cracks and damage to nearby buildings. In such situations, the prediction, monitoring and control (Colaço *et al*., 2023) of vibrations due to pile driving are important issues to reduce or prevent pernicious effects induced by this construction activity.

In terms of prediction procedure, and given the

Correspondence to: A. Colaço, CONSTRUCT-FEUP, University of Porto, Rua Dr. Roberto Frias, 4200-465 Porto, Portugal
Tel: +351-225 081 814
E-mail: aires@fe.up.pt

† PhD Researcher; ‡Professor ; §Engineer

Supported by: Programmatic funding - UIDP/04708/2020 of the CONSTRUCT - Instituto de I&D em Estruturas e Construções - funded by national funds through the FCT/MCTES (PIDDAC); Project PTDC/ECI-CON/29634/2017 - POCI-01-0145-FEDER-029634 - funded by FEDER funds through COMPETE2020 - Programa Operacional Competitividade e Internacionalização (POCI) and by national funds (PIDDAC) through FCT/MCTES. Grant No. 2022.00898. CEECIND (Scientific Employment Stimulus - 5th Edition) provided by ‘‘FCT– Fundação para a Ciência e Tecnologia”

Received April 14, 2022; **Accepted** January 4, 2023

complexity of the entire system involved, the first studies on ground vibration induced by pile driving were based on empirical approaches (Attewell and Farmer, 1973; Attewell *et al*., 1992; Whyley and Sarsby; 1992, Massarsch and Fellenius, 2008, 2015; Cleary and Steward, 2016; Grizi *et al*., 2018). More recently, some authors have addressed this problem from a numerical point of view: Ramshaw *et al*. (2001) and Khoubani and Ahmadi (2014) proposed an axisymmetric model based on finite-infinite elements for the simulation of the pile-ground system. A similar modelling technique, but using artificial boundaries based on a gradual increase of soil damping to simulate Sommerfeld′s condition, was presented by Homayoun Rooz and Hamidi (2019). Following a similar strategy for the treatment of artificial boundaries, Sofiste *et al*. (2020) recently proposed a computational model based on explicit time domain analysis. Taking into account that the soil strain levels in the vicinity of the pile are high, thus inducing nonlinear soil behavior, Masoumi *et al*. (2009) presented a nonlinear coupled finite element-boundary element approach for the prediction of free field vibrations due to vibratory and impact pile driving. Also including the nonlinear behavior of the soil, Grizi *et al*. (2018) used the commercial software Plaxis 3D to compute vibration fields induced by impact pile driving. The results from an explicit element analysis, including an animated simulation of the pile driving process, can be found in Zhao and Lin (1996).

From the literature, it is clear that the nonlinear behavior of the soil close to the pile plays a relevant role in the generated vibration field. On the other hand, nonlinear analyses are not suitable to be performed in the frequency domain, demanding time-domain schemes that are usually challenging from the points of view of computation efficiency and mathematical complexity. Thus, in the present study, a frequency domain dynamic model based on finite element method (FEM) is proposed, with the following procedures: i) coupling the FEM domain with perfectly matched layers, to avoid spurious reflections in the domain truncation boundaries; and ii) matching the soil properties as a function of the strain level, i.e., performing an equivalent linear analysis to consider the consequences of the nonlinear behavior of the soil close to the pile. The combination of these two procedures allows for the creation of an efficient and robust prediction tool, avoiding the need to employ more advanced soil constitutive models or complex techniques to solve the dynamic equations of equilibrium in the time domain.

Since the experimental validation of the proposed numerical approach (described in Section 2) is a mandatory step to create a reliable prediction tool, a comprehensive experimental test site was implemented in the residual soils from Porto granite. The experimental testing program can be grouped into two distinct components: i) geotechnical investigation and soil testing; and ii) measurement of vibrations induced by pile driving. Both components are described in Section 3 of the present paper. Section 4 is dedicated to the experimental validation of the proposed prediction model, where the simulated results are compared with the experimental measurements. In Section 5, the main conclusions and findings derived from this study are summarized.

Thus, the goal of the present paper is twofold: the proposal and experimental validation of a fully integrated prediction numerical model; and the description and characterisation of a comprehensive experimental test site. The latter represents a relevant output for the technical and scientific communities dealing with the subject of vibrations induced by pile driving, since the experimental database, available as supplemental data, can be used by other authors on the experimental validation of prediction models.

2 Numerical prediction model

2.1 Overview

The prediction of ground-borne vibration induced by pile driving involves modelling a complex system, composed of distinct components: hammer device, pile and soil. A schematic illustration of the problem is presented in Fig. 1. To address the global system, a modular numerical model, based on a substructuring approach, is considered. This numerical model is split into two main modules: one comprises the pile-ground model, modelled by a finite element method-perfectly matched layer (FEM-PML) approach in axisymmetric conditions; the other refers to the dynamic simulation of the hammer device. Since there is a dynamic interaction problem between the hammer device and the remaining system, both models are coupled, fulfilling the equilibrium and compatibility requirements.

2.2 Modelling the pile-ground system

2.2.1 General formulation

The dynamic response induced by pile driving is

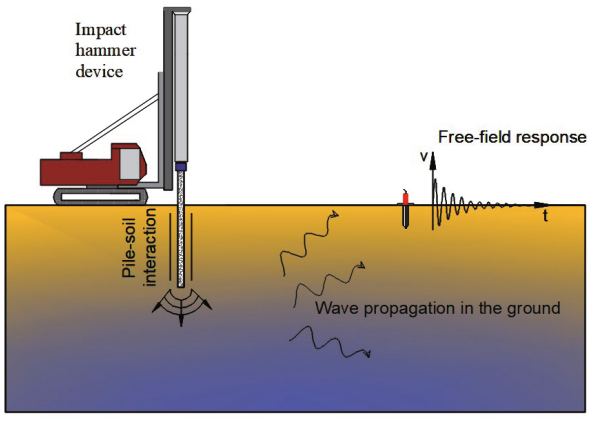

Fig. 1 Schematic illustration of the problem

computed herein by a numerical procedure based on the coupling between the finite element method and perfectly-matched layers in order to fulfil Sommerfelds′s radiation condition (Kausel, 1988; Mesquita and Pavanello, 2005). A complete description of the model can be found in Mont′Alverne Parente *et al*. (2019) and Colaço *et al*. (2020).

For computational efficiency, an axisymmetric model was assumed at the centerline of the pile, allowing the three-dimensional problem response to be obtained without the need for a 3D discretization. According to the classic finite elements notation, the dynamic pile-ground solution, in the frequency domain, can be obtained by solving the system of equations presented in Eq. (1).

$$\left[\left(\boldsymbol{K}+\boldsymbol{K}^{*}(\omega)\right)-\omega^{2}\left(\boldsymbol{M}+\boldsymbol{M}^{*}(\omega)\right)\right]\boldsymbol{u}(\omega)=\boldsymbol{p}(\omega) \quad (1)$$

where $\boldsymbol{K}$ and $\boldsymbol{K}^{*}$ are the stiffness matrices of the FEM and PML regions, respectively. $\boldsymbol{M}$ and $\boldsymbol{M}^{*}$ stand for the mass matrices of the FEM and PML regions, respectively.

Since the problem is formulated in the frequency domain, it is possible to compute transfer functions between the response and a unitary loading condition for distinct frequencies. This procedure is appealing because the response can then be scaled as a function of the loading condition.

2.2.2 Equivalent linear formulation

The assumption of a (visco-)elastic and linear behavior of the pile-ground system is a necessary condition for the development of a model in the frequency domain, as previously considered. However, this approach is a simplification of the real behavior of the soil, which is strongly dependent on the induced strain level. With the increase of the strain level, the stiffness tends to decrease and the energy dissipation tends to increase, as illustrated in Fig. 2 for a symmetric cyclic loading condition (Hardin and Drnevich, 1972).

Pile driving operations can induce strain levels in the soil larger than the elastic compatible limit. Thus, when large strains, i.e., above 10^{-4}, are expected, an equivalent linear analysis can be hereafter integrated into the modelling approach, allowing for the consideration of the effects of nonlinear soil behavior. This technique involves an iterative method, which compensates for the inelastic behavior by adjusting elastic material parameters for the corresponding strain levels. The existence of laws describing stiffness degradation and damping increase with the increase of strain levels is a key feature for enabling this iterative technique. These laws should be obtained from laboratory tests or, in their absence, from correlations with relevant physical properties of the soil (Vucetic and Dobry, 1991; Ishibashi and Zhang, 1993).

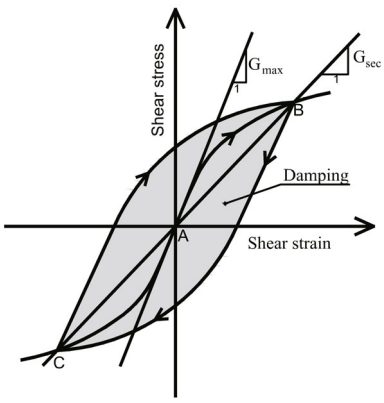

Fig. 2 Stress-strain path during cyclic loading (Costa *et al*., 2010)

As implied, the definition of the strain level at each finite element is required. In 3D problems, the strain level is usually defined by the effective octahedral shear strain, as proposed by Lysmer *et al*. (1974) and Halabian and Naggar (2002):

$$\gamma_{\text{eff}}=\alpha\frac{1}{3}\sqrt{\left(\varepsilon_z-\varepsilon_r\right)^2+\left(\varepsilon_r-\varepsilon_\theta\right)^2+\left(\varepsilon_z-\varepsilon_\theta\right)^2+6\left(\gamma_{zr}\right)^2} \quad (2)$$

where α is a parameter in the range between [0.5–0.7] (in this work, α is assumed to be equal to 0.65). The variables γ_{zr} and ε_i correspond to the strains in the strain tensor. In terms of the numerical process, and for a discretized medium through an element-by-element procedure, it is possible to determine the induced strain at each element and to make the correction of the element properties until a match is obtained with the involved strains. In the present model, it is assumed that the properties are constant inside each finite element, which means that the strains in the center point of each element are considered representative of the strains in the entire element. For the update of the properties of the elements, a set of linear problems is successively solved until a match between the strain level and the dynamic properties of the soil is reached. The procedure can be summarized as:

(1) Assume low-strain properties for all elements of the medium.

(2) Compute the time history of strains and evaluate the maximum value of γ_{eff}^{i} for each element.

(3) Use the value of γ_{eff}^{i} to choose new equivalent linear values, G_{sec}^{i+1} and ξ_{sec}^{i+1}, for the next iteration.

(4) Repeat steps 2 to 3 until the differences between shear modulus and damping in two successive iterations are below a pre-established tolerance for all finite elements.

In terms of the convergence tolerance, a value of 3% is, in the authors′ opinion, considered acceptable, since the linear equivalent model corresponds to an approximation to the real problem.

2.3 Hammer model and hammer-pile interaction

An analytical model of the impact hammer device, originally proposed by Deeks and Randolph (1993), was applied to determine the hammer impact force generated

at the top of the embedded pile. Thus, to estimate the pile head force, the impact hammer system can be simulated as a two-degree-of-freedom model, as depicted in Fig. 3.

In the frequency domain, and considering a pseudo-force application equal to the modulus of the momentum transferred from the ram to the pile ($m_r v_0$), the ram and the anvil displacement values can be computed by solving the following system of equations:

$$(-w^2\begin{bmatrix} m_r & 0 \\ 0 & m_a \end{bmatrix} + iw\begin{bmatrix} c_c & -c_c \\ -c_c & c_c \end{bmatrix} + \begin{bmatrix} k_c & -k_c \\ -k_c & k_c + k_p \end{bmatrix}) \times \begin{bmatrix} u_r \\ u_a \end{bmatrix} = \begin{bmatrix} m_r v_0 \\ 0 \end{bmatrix} \quad (3)$$

Therefore, the pile head force in the frequency domain is obtained by the product between the pile dynamic stiffness, k_p (computed by the axisymmetric FEM-PML model assuming a unitary load applied at the pile head), and the anvil displacement, u_a.

When the ram impacts the anvil surface, the soil resistance slows the pile movement and causes the ram to rebound. Since the anvil surface force is achieved by assuming a linear elastic model, tractions are generated at the moment of the ram rebound. This effect is due to a weakness of the models since the loss of contact between bodies cannot be represented, due to its elastic nature. To prevent these tractions and hence the rise of negative forces, the anvil surface force in the time domain is truncated.

After computing the load applied at the pile head, the dynamic response of the system is obtained, in the frequency domain, through the multiplication of the transfer function by the loading function. Results in the time domain are then obtained by an inverse Fourier transform operation.

3. Experimental test site

3.1 General description

The experimental test site was implemented near the city center of Porto (Portugal), where a building founded in piles was under construction at the time of the experimental campaign. The building plan consists of a ten-storey reinforced concrete structure, with a total plan area of about 1200 m^2. The building also comprises one underground floor for parking. The general view of the test site at the time of pile driving is depicted in Fig. 4.

Concerning the building foundations, a total of 156 square piles were driven, with two distinct sections of 400 mm × 400 mm and 350 mm × 350 mm. The piles have a total length varying between 8 and 15 m, as a function of the geotechnical conditions of the site. The foundation plan is depicted in Fig. 5. These driven piles are made from precast concrete, with Young's modulus, E, around 30 GPa and mass density, ρ, of 2500 kg/m^3. A hysteretic damping factor equal to 0.01 was considered for the pile and the value of 0.15 for the Poisson's ratio.

3.2 Geotechnical characterization

3.2.1 In-situ tests

According to the geological-geotechnical report that supports the building design, a total of seven boreholes, with standard penetration test (SPT) tests spaced every 1.50 m in depth, were carried out. The boreholes were drilled from the ground surface before the excavation, of around 3 m, for the elevation of the underground floor. Essentially, the site is geologically formed by a granite residual soil, with a typical increase of stiffness and strength with depth, as can be seen in Fig. 6. The groundwater table was found at a depth of approximately 8 m (from the base of the excavation).

Despite the relevance of the results provided by the geological-geotechnical report, the information is more qualitative than quantitative for the problem of vibration propagation, since those tests involve high-strain deformation levels, incompatible with the small-strains usually induced by pile driving operations, particularly at large distances from the pile. Thus, during the initial phase of the construction, non-intrusive geophysical tests, such as seismic refraction tests (SRT) and spectral analysis of surface waves (SASW) tests were performed. These geophysical tests include an experimental component as

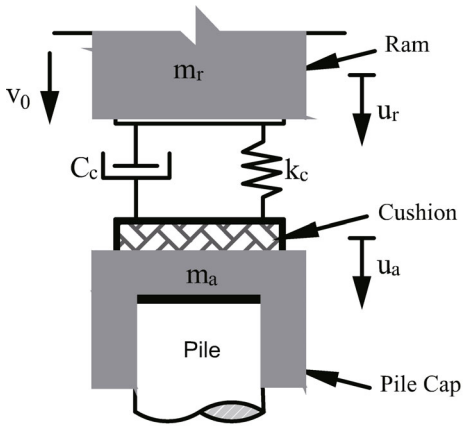

Fig. 3 Two degrees-of-freedom pile-hammer model

Fig. 4 General view of the experimental test site

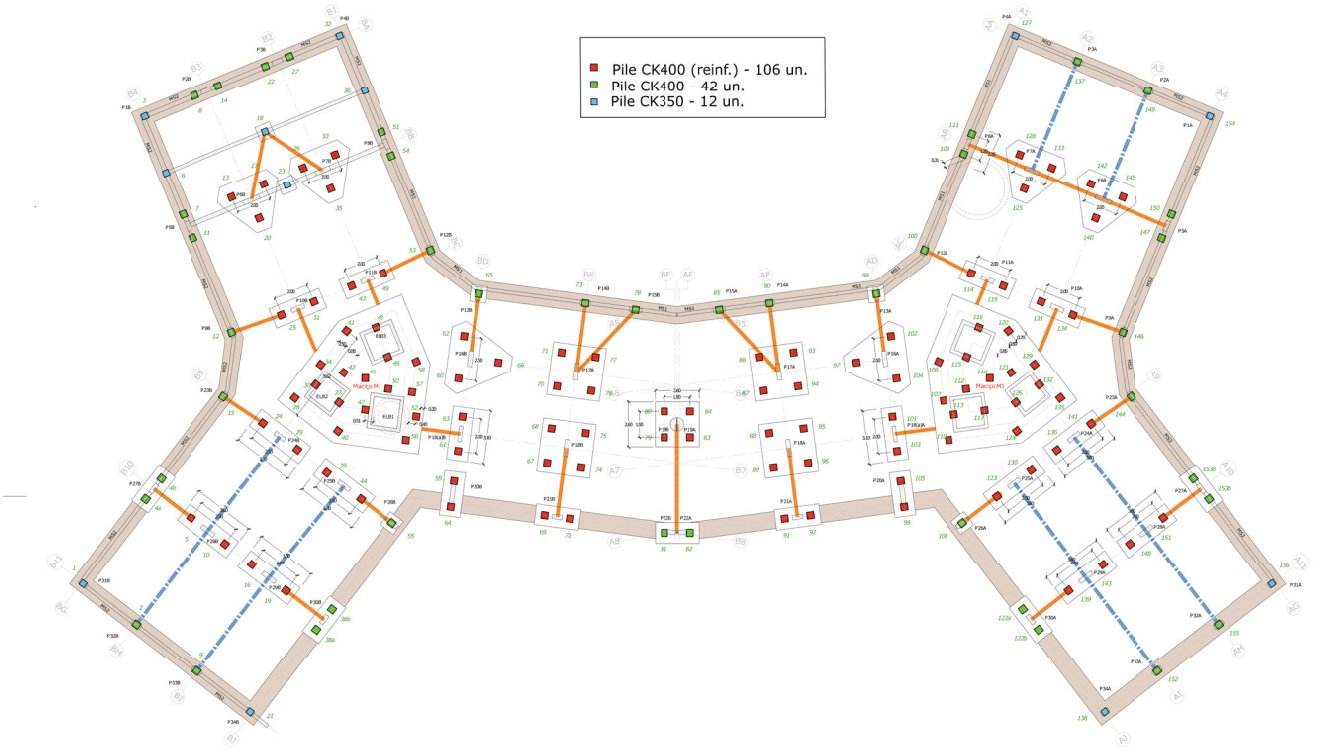

Fig. 5 Foundations plan

well as a numerical procedure. The experimental part consists of the application of an impulse force on the ground surface and the recording of the transient signal using accelerometers placed along a straight line starting from the impulse location (Fig. 7).

From the seismic refraction tests, the P-wave velocity is directly obtained from the time-domain analysis of the results recorded for each position and the S-wave velocity is obtained by an inversion procedure taking into account the experimental P-SV dispersion relationship shown in Fig. 7. Additional details about the mathematical formulation can be found in Degrande *et al*. (2008).

The obtained P and S-wave velocity profiles are presented in Fig. 8. Laboratory characterization of the soil indicates a mass density close to 1900 kg/m^3. As expected, a large increase in the P-wave velocity occurs at the depth of the groundwater table. According to the sensitivity study preconized by Colaço *et al*. (2022), a hysteretic damping factor of 5% is admitted for the first layer and a value of 2.5% for the remaining layers. In more detail, the adopted hysteretic damping factors were estimated, based on the results from a previous low-strain test. This test consists of applying an impulse force on the pile head, previously installed on the ground, using an instrumented hammer, as the transient signal recorded using unidirectional accelerometers placed in a straight line starting from the pile′s location (a total of 50 measurement points was considered, equally spaced over 50 m). The hysteretic damping factors were obtained by an inversion procedure, in which the experimental results were compared with those provided

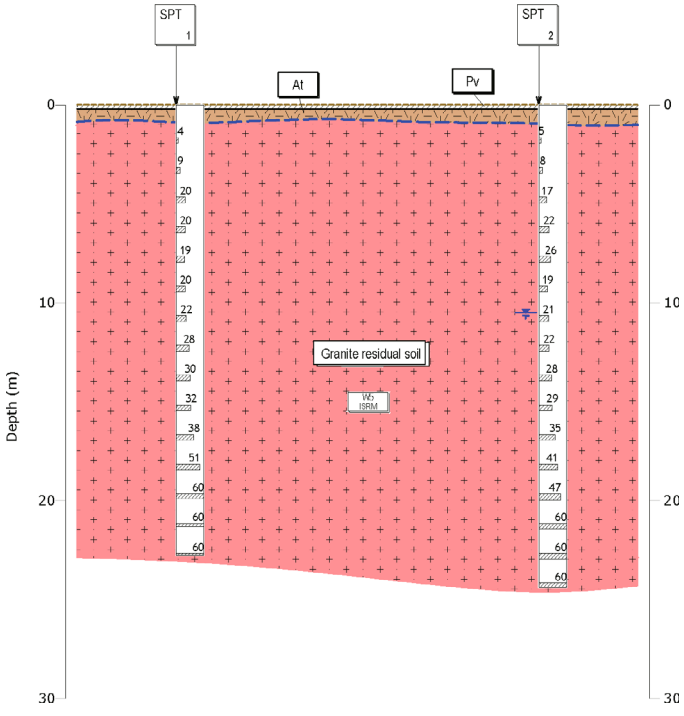

Fig. 6 Geological-geotechnical profile

by the numerical simulations, to derive the best estimate of the hysteretic damping.

In addition to the non-intrusive geophysical tests, the results provided by two cross-hole tests (CH) performed at the same site were also considered in the dynamic characterization of the soil. These tests were performed

within the scope of a previous research project on the geomechanical characterization of these granite residual soils.

When comparing the results given by the non-intrusive geophysical tests and by the cross-hole tests depicted in Fig. 8, some differences are found. These differences were expected and may be explained by the different locations where the in-situ tests were performed, the heterogeneity of the ground, as well as the region covered by each test. In fact, SASW tests involve a larger volume of the ground, while cross-hole tests provide information corresponding to a more restricted region. However, the main reason that justifies the differences found on the S- and P-wave profiles is that the cross-hole tests were performed before excavation and the SASW tests were performed at the ground surface after excavation of around 3.5 m of granite residual soil (for the construction of the underground floor). Thus, the excavation induced stress is relieved on the ground with the consequent reduction of soil stiffness.

3.2.2 Laboratory tests

In addition to small-strain stiffness data, the dynamic modelling of the wave propagation induced by pile driving demands information about the stress-strain soil behavior when the strains are larger than the elastic threshold. Such information can only be obtained from advanced laboratory tests performed on high-quality soil samples. This aspect was addressed in a previous research project on the characterisation and behavior of residual soils, where soil samples collected at the same site were investigated (Fonseca *et al.*, 2006, Ferreira *et al.*, 2007; Ferreira, 2009). The laboratory-testing

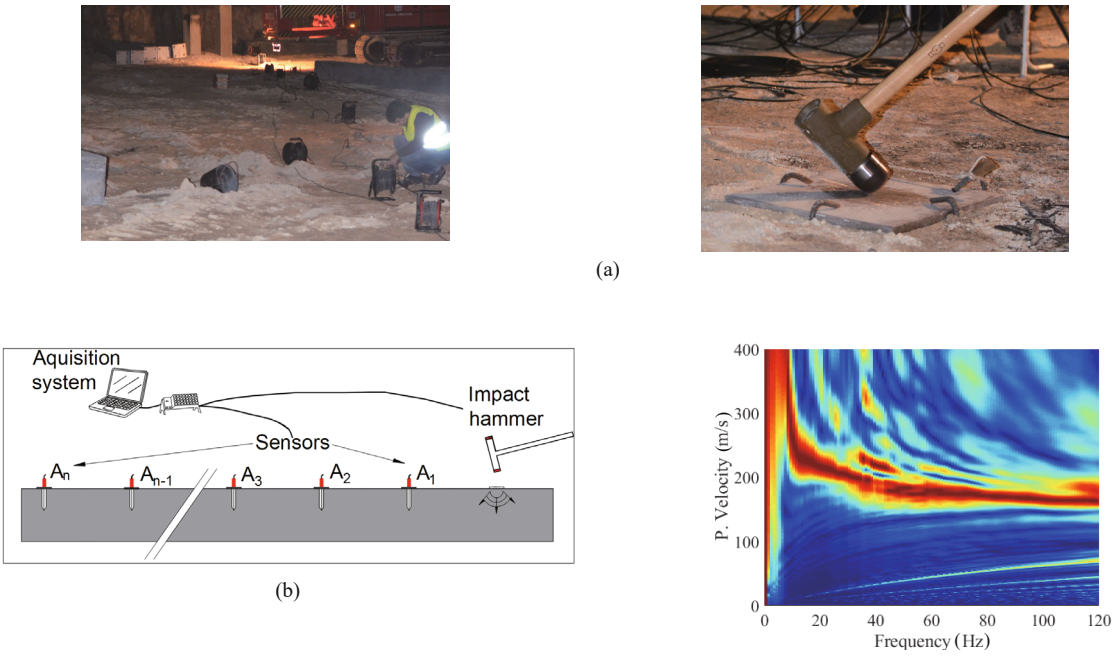

Fig. 7 Dynamic characterization of the soil: (a) photos of in situ testing activities; (b) setup for the experimental activities; (c) experimental P-SV dispersion relationship

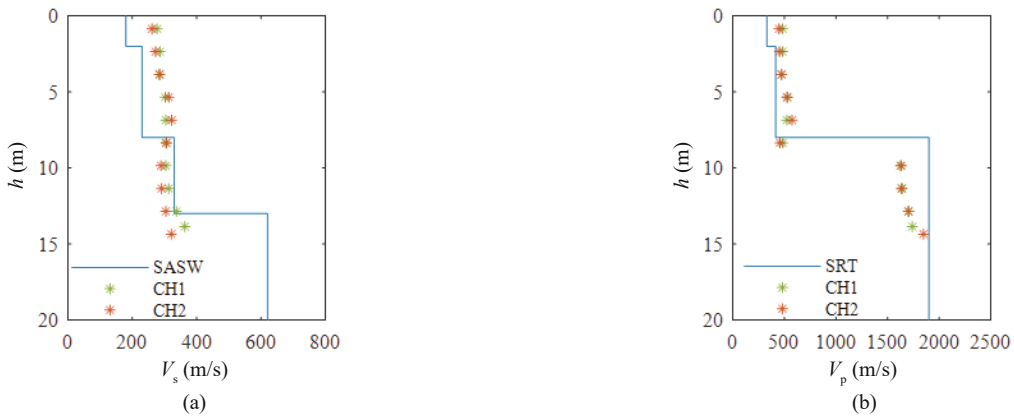

Fig. 8 Dynamic properties of the soil with depth: (a) S-wave velocity profile; (b) P-wave velocity profile

program included numerous triaxial tests with seismic wave measurements and resonant-column (RC) tests. An example of a soil sample of this site and its preparation for resonant-column testing is presented in Fig. 9.

The resonant-column apparatus used for this work is a Hardin-type oscillator, installed at the geotechnical laboratory of the Technical University of Lisbon (IST). In these tests, a torsional vibration is applied to the cylindrical soil specimen in the form of continuous sine excitation. At each testing stage, the input frequency is gradually increased until resonance is reached. Under the resonant condition, the main parameters are recorded, namely the resonant frequency, current, output amplitude and specimen displacement. From these measurements, the shear strain, shear modulus, damping ratio and void ratio are automatically computed.

The RC tests were carried out in isotropic and anisotropic consolidation conditions, at various stages, on natural intact soil samples collected from the experimental site. This residual soil is usually defined in the unified classification of soils (ASTM D 2487-85), as silty (SM) or well-graded (SW) sands. The grading characteristics of the tested samples are D_{50}=0.22–0.25, C_u=100–160 and C_c=0.4–1.4. The presence of fines adds higher compressibility than that of sands, though permeability is relatively high (k=10^{-6}–10^{-5} m/s). Further details of the laboratory physical and mechanical characterization of this soil can be found elsewhere (Ferreira *et al*., 2007, 2011; Ferreira, 2009). All tests were performed in drained conditions, with the samples at the natural moisture content, for a direct comparison with the in-situ state. At each loading stage, the RC measurements were taken after consolidation at constant volume. The main physical properties of the natural specimens are summarized in Table 1, including unit weight (γ), water content (w), degree of saturation (S_r), initial void ratio (e_0), and coefficient of earth′s pressure (K_0). The RC testing conditions of each specimen are also included in Table 1, namely mean effective stress (p') and maximum shear strain (max ε_s).

After the consolidation stages, these samples were subjected to increasing levels of shear strain, to determine the stiffness degradation and damping curves, as shown in Fig. 10. These graphs show the reduction of the stiffness modulus as a plot of G/G_0 versus shear strain, where G_0 is the elastic, or very small-strain, shear modulus (e.g., Fahey, 1992). Figure 10(b) illustrates the obtained damping ratios, which increase with shear strain.

In terms of the equivalent linear methodology, the existence of a mathematical law describing stiffness degradation and damping increase with the increase of the strain levels is the ideal condition. As such, the laws proposed by Ishibashi and Zhang (1993) are also plotted in Fig. 10 for the same conditions as the laboratory tests (different confining stresses and considering PI=0).

Fig. 9 Soil specimens for RC testing

Table 1 Testing conditions and physical characteristics of RC intact specimens

Specimen	Depth (m)	γ (kN/m^3)	w (%)	S_r (%)	e_0	K_0	p' (kPa)	max ε_s
S5-1-RC	4.10	20.0	13.8	77	0.497	0.5	53.3	2.5×10^{-4}
S5-2-RC	8.60	19.0	19.7	83	0.663	0.5	106.7	3.9×10^{-4}
B5-1-RC	4.15	15.4	16.9	49	0.994	0.35	283.3	6.7×10^{-4}
B5-2-RC	4.15	15.4	16.9	49	0.994	0.35	60.0	8.0×10^{-4}

3.3 Experimental assessment of vibrations induced by pile driving

The ground motion measurements presented along the current section include the excitation induced by the driving of four piles: three of them with a section of 400 mm × 400 mm and another one with 350 mm × 350 mm. All piles have a total length equal to 12 m. During the driving operations, the hammer height-of-fall is variable, increasing with the increase of the penetration depth (from 15 cm to a maximum of 60 cm). The driving equipment corresponds to a Junttan PMx25 equipped with the hydraulic impact hammer SHK110-7. The mass of the hammer ram is equal to 7 t. The transient signal is recorded at the ground surface for a wide range of points, placed between 1 m and 32 m from the pile. Figure 11 presents photos of the driving equipment and the unidirectional accelerometers used to record the ground response.

Generally, it is possible to systematize the extended set of information recorded through a scatter plot, where the peak particle vertical velocity of vibration is plotted as a function of the distance to the vibration source, i.e., to the pile. This result has a high practical value, allowing the identification of the maximum peak vibration velocity, expected at the level of the building foundations located in the vicinity (if the SSI conditions allow neglecting the kinematic interaction). In this case, the values evaluated for the set of measurement points and different pile penetration depths are represented through the scatter plot in Fig. 12. In this regard, it should be clarified that a separation of the events (impacts) was made for each meter of driving, allowing the adoption of average values for each driving interval.

From the obtained results, it is possible to verify the prevalence of peak particle velocity maximums around 200 mm/s in the vicinity of the pile, and 20 mm/s for a distance of 10 m from the pile. This value is reduced to values below 5 mm/s for distances higher than 30 m.

Despite the significance of this information, the PPV values should be analyzed taking into account the range of the most relevant frequency content of the response. In fact, the standards that address this issue typically impose limits on the peak value assessed near building foundations; this limit value is variable, according to the predominant frequency in the velocity spectrum. Considering the results obtained during the driving of one of the monitored piles with a 400 mm × 400 mm

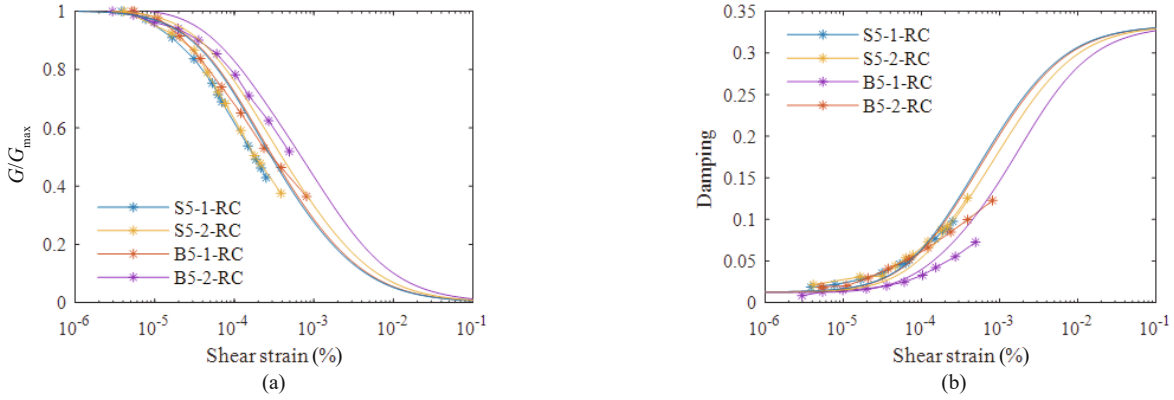

Fig. 10 Evolution of the dynamic properties of a granite residual soil with shear strain: (a) stiffness degradation; (b) damping increase (resonant column results and Ishibashi and Zhang curves (1993))

Fig. 11 Experimental test site: (a) pile driving rig Junttan PMx25 equipped with the hydraulic impact hammer SHK110-7; (b) and (c) unidirectional accelerometers placed along the ground surface

cross-section, the frequency content has been computed for three points placed at different distances from the pile, namely 8, 16, and 32 m, as shown in Fig. 13. In the same figure, time-domain records are also presented.

As evidenced by the curves illustrated in Fig. 13, and in addition to the expected attenuation of peak velocity values with increasing distance, there is an attenuation of the response at higher frequencies. This fact derives from the larger influence of the material damping in the higher frequency content attenuation.

Another interesting aspect corresponds to the evolution of the frequency content with the increase of pile penetration depth. Although the hammer height-of-fall is variable, the focus here is on the range, instead of the amplitude, of the dominant frequencies. Thus, Fig. 14 presents three curves corresponding to pile penetration depths in the intervals [2–3] m, [5–6] m, and [8–9] m, for distances of 8 and 24 m to the pile. As can be seen, no significant variation in the frequency content can be observed with increasing driving depth.

This experimental setup allowed the recording of the radial velocity component at two points: 4 m and 12 m away from the pile. This information is useful for the analysis of the particle trajectories, where the vertical and radial velocities are plotted against each other, as depicted in Fig. 15. The analysis of the motion paths allows verifying that the main motion component is the vertical direction, although the difference is not very significant. This means that for this event, where the pile tip is located at about 2 m depth, the vibration measured in the points located at 4 m and 12 m away from the source is dominated by the propagation of P-SV surface waves (Massarsch and Fellenius, 2008).

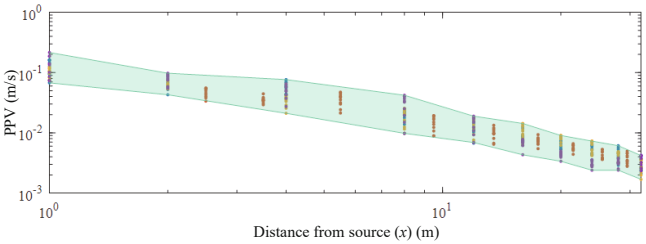

Fig. 12 Experimental results: peak particle velocity versus distance from the pile

4 Numerical comparison and experimental validation of the numerical model

4.1 Initial considerations

As initially established, the experimental validation

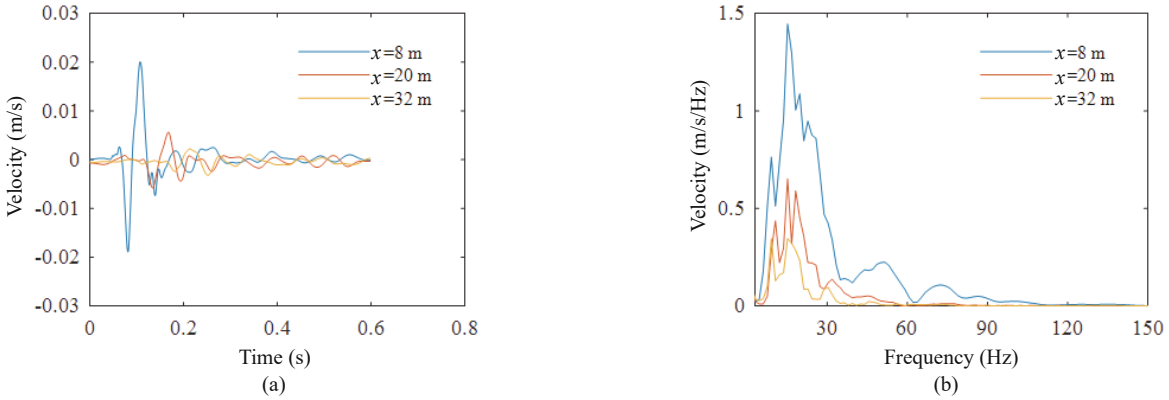

Fig. 13 Experimental vertical vibration velocities measured at different distances from the pile and for a penetration depth in the interval 5–6 m: (a) time-history; (b) frequency content (*r*=8, 20 and 32 m)

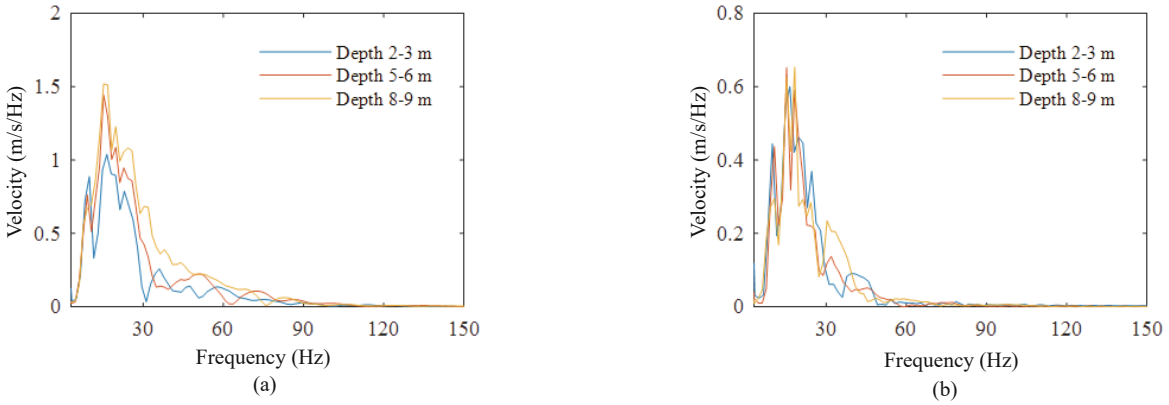

Fig. 14 Frequency content of the experimental vertical vibration velocities considering different pile penetration depths: (a) *r*=8 m; (b) *r*=24 m

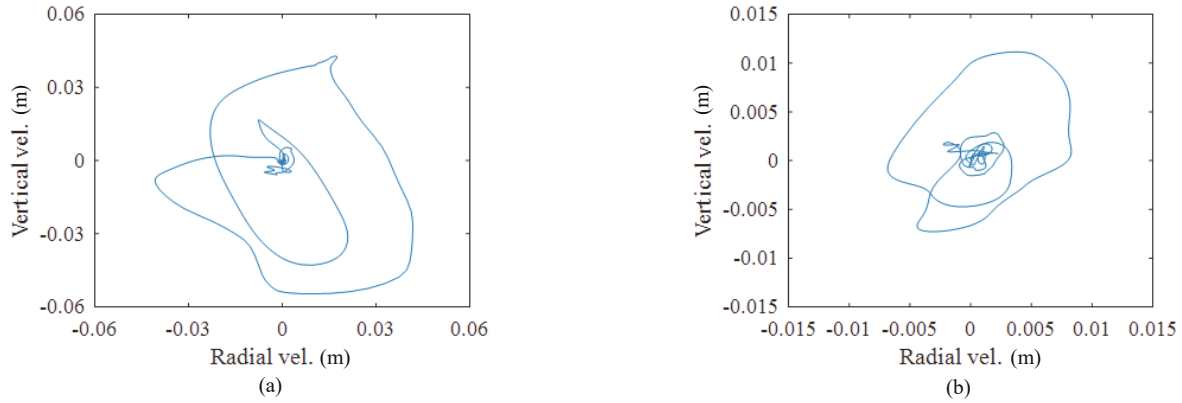

Fig. 15 Particle trajectories in the observation points at: (a) x=4 m; (b) x=12 m (pile penetration depth in the interval 2–3 m)

of the implemented numerical model is one of the main objectives of the presented work. Thus, the pile-ground elastodynamic properties initially defined were used in the numerical simulation of the case study. Given the limitations of an axisymmetric formulation, in which it is not possible to model the true geometry of the pile (square section of 400 mm × 400 mm), an equivalent circular pile section was considered. As a general overview, the pile-ground medium is discretized by an FE-PML mesh with 36,639 triangular elements with 6 nodes (a total of 71,665 nodes), corresponding to a discretized cross-section of 35 m × 25 m. Taking advantage of the axisymmetric formulation conditions, the problem is solved as a two-dimensional problem where the pile centerline axis corresponds to the axisymmetric axis. The PML layers are bounding the FEM region, as illustrated in Fig. 16.

In terms of the driving device, the following parameters were adopted: m_a=850 kg; m_r=7000 kg, k_c=2 × 10^6 kN/m and c_c=6 × 10^5 kN·s/m. Regarding the impact velocity of the ram, v_0, a short explanation is necessary: theoretically, the potential energy, $E_p = m_r g h$, is assumed to be equal to the kinetic energy, $E_c = m_r v_0^2 / 2$. From this relation, it is possible to relate the hammer height-of-fall (experimental data) with the velocity of the ram. However, in practical applications, it is necessary to take into account the energy loss during the process of hammer fall. Thus, a coefficient of restitution, α, of 0.75 was considered: $E_c = \alpha E_p$. Note that the adopted value was selected based on a sensitivity analysis, where the influence of this factor was investigated through the comparison between experimental and numerical results; for this reason, some preliminary analyses are recommended for different applications, especially when dealing with different pile-driving equipment.

Since the equivalent linear approach is a simplified method to simulate the nonlinear soil behavior, the authors have compared the numerical response with a fully nonlinear soil model. In this case, the hardening soil model with small-strain stiffness (Hssmall) was

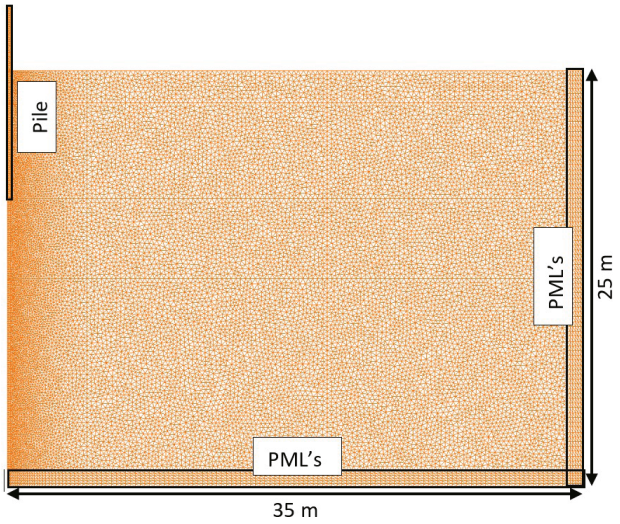

Fig. 16 FE–PML mesh adopted to model the pile-ground system

used in an axisymmetric numerical model formulated in the time-domain. For this purpose, the software Plaxis (Brinkgreve *et al.*, 2019) was used. The mesh adopted is shown in Fig. 17. The numerical model is made up of 24,326 elements and 49,075 nodes. Triangular elements (6-node elements) were used for area elements. The boundary conditions correspond to viscous dampers (Lysmer and Kuhlemeyer, 1969) in all boundaries except at the plane of symmetry, where horizontal movements are hindered, and at the ground surface, which is a free boundary.

The time step was selected to ensure that a wavefront does not move during a single step at a distance larger than the minimum dimension of an element ($l_{e,\min}$). In this case, the stiffest element used in the 2D axisymmetric numerical model corresponds to the pile, which determines the critical time step. This is computed as $l_{e,\min}/V_p$, which in this case is equal to 2.5 × 10^{-5} s.

In Table 2, the soil parameters in the HSsmall model are shown.

4.2 Numerical comparison and experimental validation

To achieve reasonable representativeness of the experimental results, four pile penetration depths were considered in the numerical results, by varying the hammer height-of-fall according to the experimental condition of the driving operations: 2 m (hammer height-of-fall of 20 cm); 5 m (hammer height-of-fall of 40 cm); 8 m (hammer height-of-fall of 50 cm) and 12 m (hammer height-of-fall of 60 cm). The envelope of the PPV with the distance to the pile obtained using the linear equivalent numerical approach is plotted over the experimental results, as can be seen in Fig. 18 (blue shade).

From the analysis of Fig. 18, it is possible to identify a good match between experimental and numerical results. In fact, the results provided by the proposed equivalent linear methodology can be interpreted as an upper limit of the experimental results. This result is particularly useful as a prediction tool, such as in the present case.

Additionally, and from a purely theoretical perspective, the numerical analysis presented above can be performed using an elastic-linear approach, i.e., neglecting the soil stiffness degradation and damping increase as a function of the strain level. The obtained results correspond to the envelope represented by a red color in Fig. 18. As previously discussed, such an approach is a simplification of the real soil behavior, since the strain levels induced in the vicinity of the pile are not compatible with this assumption. From the figure, it can be seen that the PPV values of the equivalent linear envelope are, approximately, three times lower than the corresponding linear envelope. However, there is an approximation trend between both attenuation laws with the increase of the distance from the source. This relation could be an important feature for a first prediction of the expected vibration levels.

Moving on to a more detailed analysis, and considering the particular case of the pile penetration depth equal to 2 m, Fig. 19 presents the comparison between the numerical and the experimental results of one of the monitored piles with a 400 mm × 400 mm cross-section. In terms of experimental results, the curves shown in this figure were obtained for pile penetration depths in the intervals [1–2] m and [2–3] m. Regarding the numerical simulation, three different curves are plotted in the same figure: two curves correspond to the results provided by the equivalent linear and linear approaches initially presented and the last one corresponds to the results obtained through the nonlinear model implemented in the software Plaxis.

Analyzing the results depicted in Fig. 19, it is possible to identify a very good match between the experimental data and the numerical results provided by the equivalent linear approach. In fact, the overall behavior of the system is satisfactorily captured by the numerical model, as expected from the previous general comparison. Results obtained with the nonlinear method confirm the suitability of the equivalent linear approach to deal with this type of problem. Indeed, a good match between the curves is accomplished for the entire measurement range.

Looking at the entire time record presented in Fig. 20, there is a satisfactory match between experimental and numerical data (equivalent linear approach), even when the observation point is far away from the impact source. In this particular case, only the experimental data

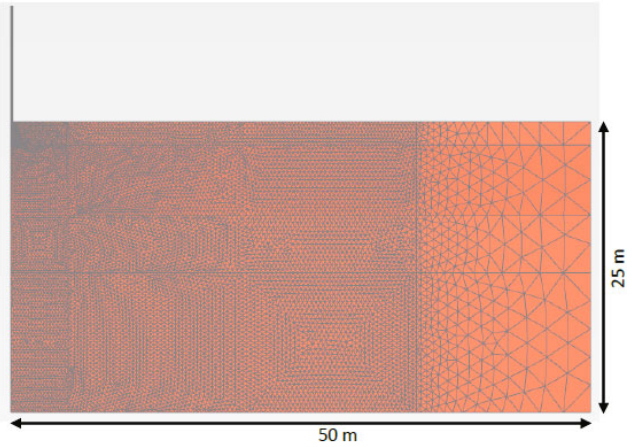

Fig. 17 Mesh adopted in nonlinear model

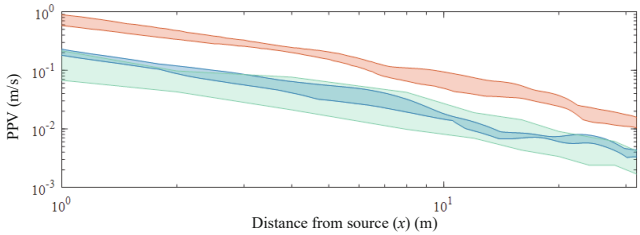

Fig. 18 Comparison between experimental and numerical results of PPV vs. distance from the pile: green shade – experimental results; blue shade – envelope of the numerical results using an equivalent linear approach; red shade–envelope of the numerical results using a linear approach

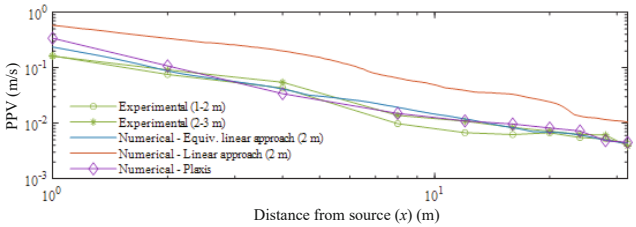

Fig. 19 Comparison between experimental and numerical results–PPV vs distance–for a pile penetration depth of 2 m

measured for the pile penetration depths in the interval [2–3] m and the numerical results from the equivalent linear approach are presented for clarity.

Despite the good agreement between experimental and numerical data in terms of peak particle values and time records, an analysis in the frequency domain is mandatory for a deeper understanding of the problem. In fact, it is not only necessary to take into account the maximum levels of vibration, but also the most relevant frequency range of the response. The numerical prediction tool should be able to correctly estimate the frequency content to constitute a reliable tool for design purposes. Following that goal, Fig. 21 presents the comparison between experimental and numerical results in the frequency domain. As can be seen, a very good agreement is reached for all observation points when an equivalent linear analysis is performed. An interesting aspect that should be highlighted refers to the frequency content results from the linear analysis, which are completely out of range with the experimental results.

Additionally, and considering a linear response of the pile-ground system, Fig. 21(a) shows the contour plot of the maximum octahedral strain level for the particular case under analysis. As shown, the pile driving operation induces strain levels in the soil above 10^{-4}, well above the typical limit generally considered acceptable for the elastic range. This region with higher strain deformation extends to a horizontal distance of around 2 to 2.5 times the depth penetration of the pile and to a vertical distance of up to 2 times the penetration depth of the pile. From these results, and after an iterative numerical scheme, Figs. 21(b) and 21(c) show an overview of the regions that are subjected to stiffness degradation and damping increase. These quantities correspond to the ratio between the final and original elastic properties (stiffness modulus and damping) of the ground.

Table 2 Soil properties in HSsmall model

	E_{50} (kN/m^2)	E_{oed} (kN/m^2)	E_{ur} (kN/m^2)	φ (°)	c (kN/m^2)	ψ (°)
Soil 1	7.5×10^3	7.5×10^3	30×10^3	30	20	0
Soil 2	20×10^3	20×10^3	70×10^3	33	35	0
Soil 3	150×10^3	150×10^3	300×10^3	35	45	0
Soil 4	550×10^3	550×10^3	1,100×10^3	40	55	0

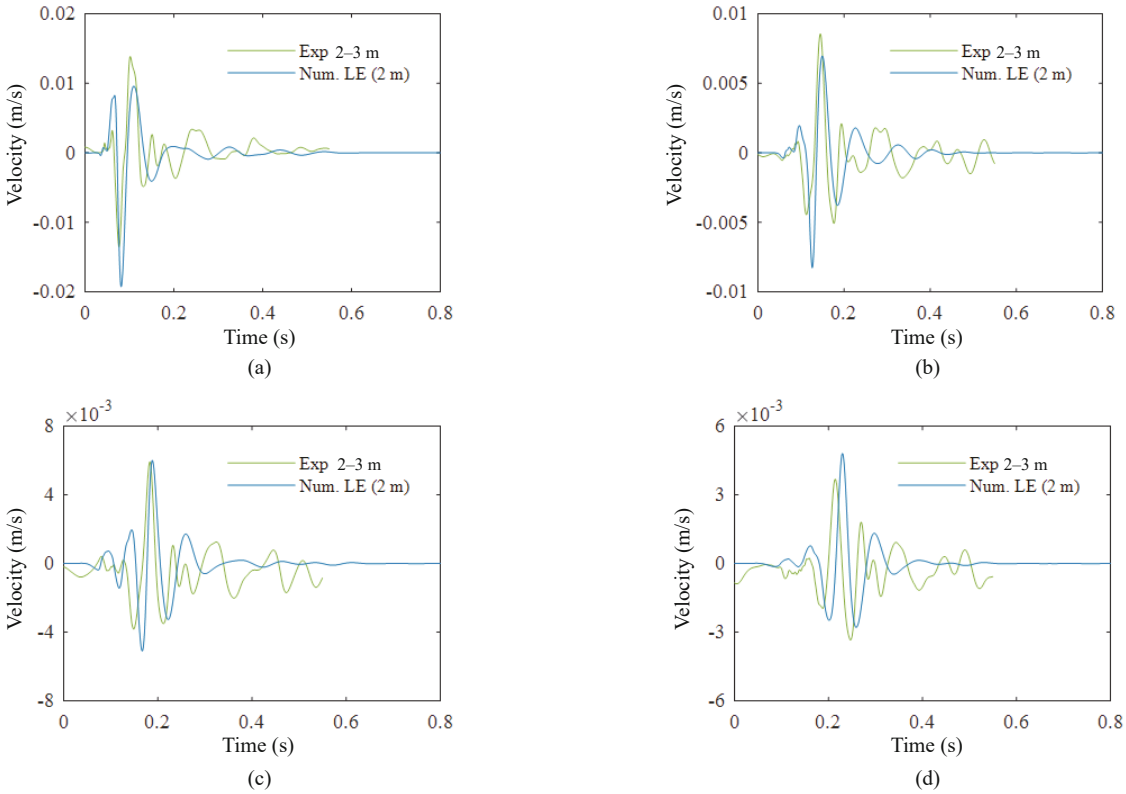

Fig. 20 Comparison between experimental and numerical time records for an observation point located at the ground surface and a distance from the pile of: (a) 8 m; (b) 16 m; (c) 24 m; (d) 32 m

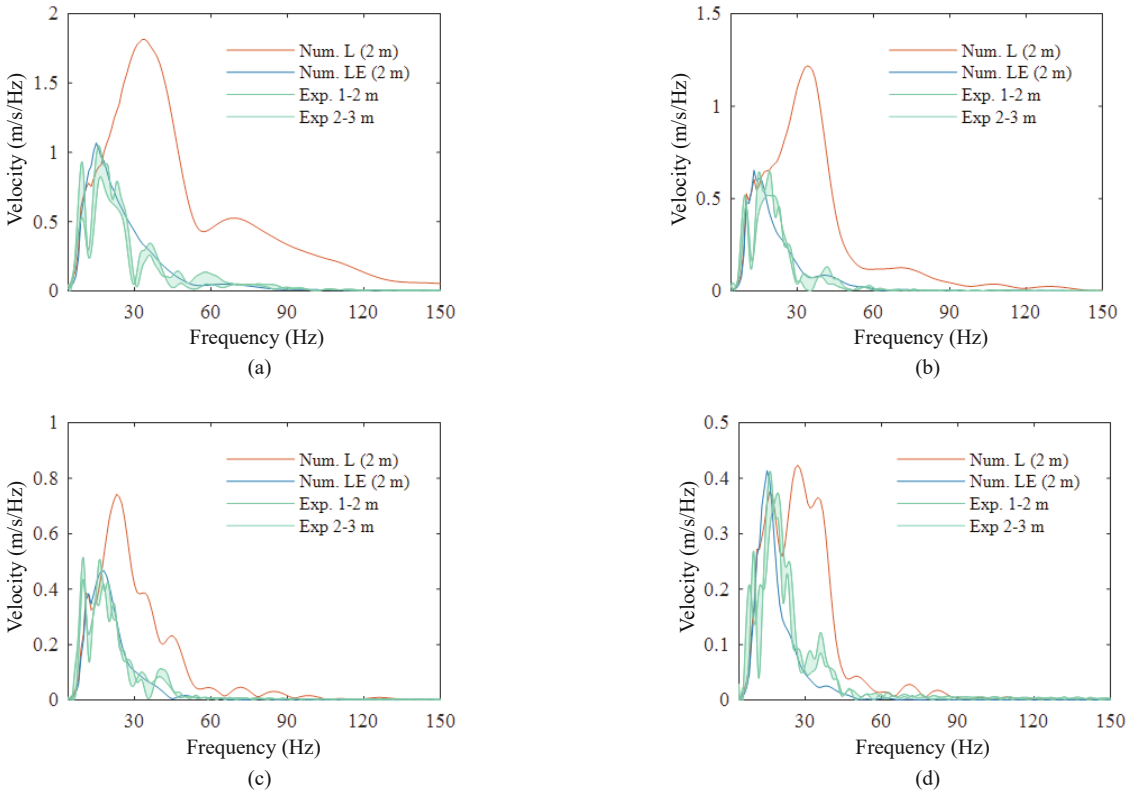

Fig. 21 Comparison between experimental and numerical results in the frequency domain for an observation point located at the ground surface and at a distance from the pile of: (a) 8 m; (b) 16 m; (c) 24 m; (d) 32 m

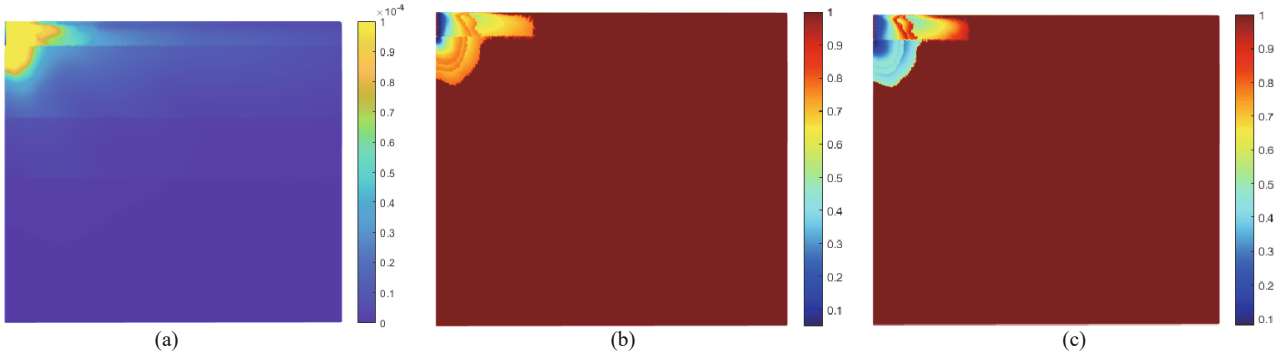

Fig. 22 Ground properties degradation: (a) octahedral shear strain; (b) E/E_0; (c) ξ_0/ξ

5 Conclusions

An equivalent linear axisymmetric FEM-PML approach for the prediction of free-field vibrations due to impact pile driving is presented herein. A subdomain approach has been used, where the numerical model is split into two main modules: the first one comprises the pile-ground system and the second one corresponds to the dynamic simulation of the hammer device. The nonlinear behavior of the ground is addressed through an equivalent linear methodology, rendering a simple but reliable methodology.

Given the complexity of the problem under analysis, the proposed numerical approach was experimentally validated. For that purpose, a comprehensive experimental test site was implemented in the residual soils from Porto granite. The experiments and tests were grouped into two distinct components: i) geotechnical investigation and soil testing; and ii) measurement of vibrations induced by pile driving. The data collected allowed the experimental validation of the numerical prediction tool, where a very good agreement was observed between the experimental data collected in those experiments and the prediction performed by the equivalent linear numerical model. Moreover, it should be mentioned that the high strain levels induced by pile driving are not compatible with an assumption of the linear behavior of the soil. In effect, the introduction of the soil stiffness (and damping) degradation in the numerical approach allowed for achieving a good match between prediction and measurement, which had not been reached when an elastic linear approach was adopted.

At last, note that the existence of a comprehensive characterization of an experimental test site represents a relevant output for the technical and scientific communities dealing with the subject of vibrations induced by pile driving, since the experimental data can be used by other authors on the experimental validation of their prediction models.

Data availability statement

The data that support the findings of this study are openly available at https://s.up.pt/s6mz.

Acknowledgment

This work was financially supported by: Programmatic funding - UIDP/04708/2020 of the CONSTRUCT - Instituto de I&D em Estruturas e Construções - funded by national funds through the FCT/MCTES (PIDDAC); Project PTDC/ECI-CON/29634/2017 - POCI-01-0145-FEDER-029634 - funded by FEDER funds through COMPETE2020 - Programa Operacional Competitividade e Internacionalização (POCI) and by national funds (PIDDAC) through FCT/MCTES. Grant No. 2022.00898.CEECIND (Scientific Employment Stimulus - 5th Edition) provided by ‘‘FCT– Fundação para a Ciência e Tecnologia”.

References

Attewell PB and Farmer IW (1973), “Attenuation of Ground Vibrations from Pile Driving,” *Ground Engineering*, **6**(4).

Attewell PB, Selby AR and O′Donnell L (1992), “Tables and Graphs for the Estimation of Ground Vibration from Driven Piling Operations,” *Geotechnical and Geological Engineering*, **10**(1): 61–85.

Auersch L and Said S (2010), “Attenuation of Ground Vibrations Due to Different Technical Sources,” *Earthquake Engineering and Engineering Vibration*, **9**(3): 337–344.

Brinkgreve S RBJK, Swolfs WM, Zampich L and Ragi Manoj N (2019), *Plaxis 2019 User Manuals*, Delft, Nethlands.

Cleary JC and Steward EJ (2016), “Analysis of Ground Vibrations Induced by Pile Driving and a Comparison of Vibration Prediction Methods,” *DFI Journal - The Journal of the Deep Foundations Institute*, **10**(3): 125–134.

Colaço A, Abouelmaty AM and Costa PA (2023), “Ground-Borne Vibrations Induced by Impact Pile Driving: Experimental Assessment and Mitigation Measures,” *Earthquake Engineering and Engineering Vibration*, **22**(1): 105–115.

Colaço A, Costa PA, Mont′Alverne Parente C and Silva Cardoso A (2020), “Numerical Modelling of Ground-Borne Noise and Vibrations in Buildings Induced by Pile Driving,” *Inter-Noise 2020*, Seoul, South Korea.

Colaço A, Costa PA, Parente C and Abouelmaty AM (2022), “Vibrations Induced by a Low Dynamic Loading on a Driven Pile: Numerical Prediction and Experimental Validation,” *Vibration*, **5**(4): 829–845.

Costa PA, Calçada R, António SC and Bodare A (2010), “Influence of Soil Non-Linearity on the Dynamic Response of High-Speed Railway Tracks,” *Soil Dynamics and Earthquake Engineering*, **30**(4): 221–235.

Deeks A and Randolph M (1993), “Analytical Modeling of Hammer Impact for Pile Driving,” *Int. J. Numer. Anal. Meth. Geomech*., **17**: 279–302.

Degrande G, Badsar SA, Lombaert G, Schevenels M and Teughels A (2008), “Application of the Coupled Local Minimizers Method to the Optimization Problem in the Spectral Analysis of Surface Waves Method,” *Journal of Geotechnical and Geoenvironmental Engineering*, **134**(10): 1541–1553.

Fahey M (1992), “Shear Modulus of Cohesionless Soil: Variation with Stress and Strain Level,” *Canadian Geotechnical Journal*, **29**(1): 157–161.

Ferreira C (2009), “The Use of Seismic Wave Velocities in the Measurement of Stiffness of a Residual Soil,” *PhD Thesis in Civil Engineering*, University of Porto, Portugal.

Ferreira C, Da Fonseca AV and Nash DFT (2011), “Shear Wave Velocities for Sample Quality Assessment on a Residual Soil,” *Soils and Foundations*, **51**(4): 683–692.

Ferreira C, Da Fonseca AV and Santos JA (2007), “Comparison of Simultaneous Bender Elements and Resonant Column Tests on Porto Residual Soil,” *Solid Mechanics and Its Applications*, **146**: 523–535.

FHWA (2016), Design and Construction of Driven Pile Foundations, *Report*, National Highway Institute, U.S. Department of Transportation, Washington, USA.

Fonseca AVD, Carvalho J, Ferreira C, Santos JA, Almeida F, Pereira E, Feliciano J, Grade J and Oliveira A (2006), “Characterization of a Profile of Residual Soil from Granite Combining Geological, Geophysical and Mechanical Testing Techniques,” *Geotechnical and Geological Engineering*, **24**(5): 1307–1348.

Grizi A, Athanasopoulos-Zekkos A and Woods RD (2018a), “H-Pile Driving Induced Vibrations: Reduced-Scale Laboratory Testing and Numerical Analysis,” *IFCEE 2018*. DOI: 10.1061/9780784481585.017

Grizi A, Athanasopoulos-Zekkos A and Woods RD (2018b), “Pile Driving Vibration Attenuation Relationships: Overview and Calibration Using Field Measurements,” *Conference of Geotechnical Earthquake Engineering and Soil Dynamics V*.

Halabian A and Naggar M (2002), “Effect of Non-Linear Soil-Structure Interaction on Seismic Response of Tall Slender Structures,” *Soil Dynamics and Earthquake*

Engineering, **22**: 639–658.

Hardin B and Drnevich V (1972a), "Shear Modulus and Damping in Soils: Design Equations and Curves," *Journal of the Soil Mechanics and Foundation Division*, **98**(7): 667–692.

Hardin B and Drnevich V (1972b), "Shear Modulus and Damping in Soils: Measurement and Parameter Effects (Terzaghi Lecture)," *Journal of the Soil Mechanics and Foundation Division*, **98**(6): 603–624.

Homayoun Rooz AF and Hamidi A (2019), "A Numerical Model for Continuous Impact Pile Driving Using ALE Adaptive Mesh Method," *Soil Dynamics and Earthquake Engineering*, **118**: 134–143.

Ishibash I and Zhang X (1993), "Unified Dynamic Shear Moduli and Damping Ratios of Sand and Clay," *Soils and Foundations*, **33**(1): 182–191.

Kausel E (1988), "Local Transmitting Boundaries," *Journal of Engineering Mechanics*, **114**(6): 1011–1027.

Khoubani A and Ahmadi MM (2014), "Numerical Study of Ground Vibration Due to Impact Pile Driving," *Proceedings of the Institution of Civil Engineers: Geotechnical Engineering*, **167**(1): 28–39.

Lysmer J and Kuhlemeyer RL (1969), "Finite Dynamic Model for Infinite Media," *Journal of the Engineering Mechanics Division*, **95**(4): 859–877.

Lysmer J, Udaka T, Seed HB and Hwang R (1974), "FLUSH: A Computer Program for Approximate 3-D Analysis of Soil-Structure Interaction Problem," *EERC Report*, 75–30. Berkeley, University of California, USA.

Masoumi HR, François S and Degrande G (2009), "A Non-Linear Coupled Finite Element-Boundary Element Model for the Prediction of Vibrations Due to Vibratory and Impact Pile Driving," *International Journal for Numerical and Analytical Methods in Geomechanics*, **33**(2): 245–274.

Massarsch KR and Fellenius BH (2008), "Ground Vibrations Induced by Impact Pile Driving," *6th International Conference on Case Histories in Geotechnical Engineering*, Arlington: 1–38, USA.

Massarsch KR and Fellenius BH (2015), "Engineering Assessment of Ground Vibrations Caused by Impact Pile Driving," *Geotechnical Engineering*, **46**(2): 54–63.

Mesquita E and Pavanello R (2005), "Numerical Methods for Dynamics of Unbounded Domains," *Computational and Applied Mathematics*, **24**(1): 1–26.

Mont′Alverne Parente C, Costa PA and Cardoso AS (2019), "Ground-Borne Vibrations Induced by Pile Driving: Prediction Based on Numerical Approach, Advances in Engineering Materials, Structures and Systems: Innovations, Mechanics and Applications," *Proceedings of the 7th International Conference on Structural Engineering, Mechanics and Computation*, Cape Town, South Africa.

Ramshaw CL, Selby AR and Bettess P (2001), "Ground Waves Generated by Pile Driving, and Structural Interaction," *International Conferences on Recent Advances in Geotechnical Earthquake Engineering and Soil Dynamics*, **3**, Missouri, USA.

Sofiste T, Godinho L, Alves Costa P and Soares Júnior D (2020), "An Effective Time Domain Numerical Model for the Prediction of Ground-Borne Vibrations Induced by Pile Driving," *Inter-Noise*, Seoul, South Korea.

Vucetic M and Dobry R (1991), "Effect of Soil Plasticity on Cyclic Response," *Journal of Geotechnical Engineering Division*, **117**: 89–117.

Whyley PJ and Sarsby RW (1992), "Ground Borne Vibration from Piling," *Ground Engineering*, **25**(4): 32–37.

Zhao ZD and Lin JQ (1996), "Animated Simulation of Pile-Driving Process," *Earthquake Engineering and Engineering Vibration*, **16**(4): 104–113. (in Chinese)